ISSN 2229-5518

Signal and Pump Power Variations of the Gain and Noise Figure of the Er/Yb Co-Doped Waveguide Amplifiers

O. Mahran[1,2], G.D.Roston[1], M.S.Helmy[1], A.A.Samir[1]

Abstract: The variations of signal and pump power of the gain and noise figure of the phosphate glass Er3+-Yb3+-co-doped waveguide amplifiers(EYCDWA) are calculated from the rate equations and the light propagation equations under the uniform dopant and the steady-state condition. The gain increases and noise figure decreases as the input power increase whereas the gain increases and noise figure increases as the signal power increase for our case of calculations. In our analysis, we have neglected the amplified spontaneous emission (ASE) and have introduced the initial energy transfer efficiency.

Index Terms— Er/Yb codoped – Gain – Noise figure – waveguide - amplifier.

1. Introduction

The erbium doped waveguide amplifiers have recently attracted a great deal of attention because of the plausibility of introducing various active elements in integrated optical circuits. These integrated optics devices require a higher concentration of erbium ions than long fibers for comparable. However, high erbium concentration will increase the number of the erbium clusters, and hence reduce the spacing between the erbium ions. In this case the overlapping between the electrons clouds of erbium ions, increasing the excited state absorption (ESA). Therefore, the clustering enhances the ESA [1]. The clustering greatly reduces the pump efficiency and degrades the gain performance. Fortunately, the rare-earth element ytterbium, exhibits a better overlapping between the Yb3+ emission spectrum and the Er3+ absorption spectrum and an intense broad absorption in the wavelength range from 800 to 1080 nm, and has a weak clustering effect and a large absorption cross-section compared to erbium, by which high ytterbium ion (Yb3+) dopant level can realized in the waveguide. This can noticeably reduce the quenching side-effect caused by high Er3+ dopant concentration [2], so the erbium-ytterbium (Er3+ - Yb3+) co-dopant can efficiently improve the gain characteristics of the waveguide amplifiers.

1 Physics Department, Faculty of Science, Alexandria University, Alexandria, Egypt.

2 Physics Department, Faculty of Science, El Jouf University, El Jouf, Sakaka,Saudi Arabia.

We choose the phosphate glass Er3+ - Yb3+ - co-doped waveguide amplifier (EYCDWA) because has attracted much attention and nowadays plays an important role in optoelectronic integrated circuits (OEICs) [3-5]. In this paper the variations of signal and pump power of the gain and noise figure of the phosphate glass Er3+-Yb3+-co-doped waveguide amplifiers(EYCDWA) are calculated from the rate equations and the light propagation equations under the uniform dopant and the steady-state condition. The gain increases and noise figure decreases as the input power increase whereas the gain decreases and noise figure increases as the signal power increase for our case of calculations. In our analysis, we have neglected the amplified spontaneous emission (ASE) and have introduced the initial energy transfer efficiency.

2. Model of Calculations

2.1. Rate and light propagation equations

Supposing N1, N2 and N3 are the Er3+ ion concentrations on the 4I15/2, 4I13/2 and 4I11/2 levels, respectively; NEr is the total Er3+ ion concentration; N4 and N5 are the Yb3+ ion concentrations on the 2F7/2 and 2F5/2 levels, respectively; NYb is the total Yb3+ ion concentration.

Under the conditions of the uniform dopant and the steady-state, the Er3+ ion and Yb3+ ion on the corresponding levels depend on the amplifier length z, i.e., Ni = Ni (z). Therefore, the multilevel rate equations for the Er3+-Yb3+ co-doped system are given by [6–8]

ISSN 2229-5518

$$\frac{dN_1}{dt} = -W_{12}N_1 - W_{13}N_1 + A_{21}N_2 + W_{21}N_2 + C_{up}N_2^2 + C_{up}N_3^2 - C_{cr}N_1N_5 \quad (1)$$

$$\frac{dN_2}{dt} = W_{12}N_1 - A_{21}N_2 - W_{21}N_2 + A_{32}N_3 - 2C_{up}N_2^2 \quad (2)$$

$$\frac{dN_3}{dt} = W_{13}N_1 - A_{32}N_3 - 2C_{up}N_3^2 + C_{cr}N_1N_5 \quad (3)$$

$$N_1 + N_2 + N_3 = N_{Er} \quad (4)$$

$$\frac{dN_4}{dt} = -W_{45}N_4 + A_{54}N_5 + W_{54}N_5 + C_{cr}N_1N_5 \quad (5)$$

$$\frac{dN_5}{dt} = W_{45}N_4 - A_{54}N_5 - W_{54}N_5 - C_{cr}N_1N_5 \quad (6)$$

$$N_4 + N_5 = N_{Yb} \quad (7)$$

Where Aij = 1/τij, τij is the lifetime between levels i and j, Cup is the cooperative up-conversion coefficients, Ccr is the Yb3+ to Er3+ cross-relaxation coefficients. W12, W21 are the signal absorption and emission rates of erbium respectively.W45, W54 are the pump absorption and emission rates of ytterbium respectively.W13 is the pump absorption rate of erbium.

The stimulated emission and absorption transition rates of signal and pump wavelength, are given by

$$W_{12} = \frac{\sigma_{12}\,\Gamma_s\,P_s}{A_c\,h\,\nu_s} \qquad W_{21} = \frac{\sigma_{21}\,\Gamma_s\,P_s}{A_c\,h\,\nu_s}$$

$$W_{13} = \frac{\sigma_{13}\,\Gamma_p\,P_p}{A_c\,h\,\nu_p}$$

$$W_{45} = \frac{\sigma_{45}\,\Gamma_p\,P_p}{A_c\,h\,\nu_p} \qquad W_{54} = \frac{\sigma_{54}\,\Gamma_p\,P_p}{A_c\,h\,\nu_p} \quad (8)$$

Where Γp and Γs are the overlapping factors of the pump and the signal light, respectively, Ac is the area of the cross-section of the amplifier, σ12(vs) and σ21(vs) are the signal absorption and emission cross-section respectively, σ13(vp) is the pump absorption cross-section, σ45(vp) and σ54(vp) are the pump absorption and emission cross-section, respectively, h is Planck's constant.

Letting Pp and Ps be the pump and signal powers in the steady state, respectively, along the EYDFA are described by the power propagation equations which are given by the following equations [1-8]

$$\frac{dP_p(z)}{dz} = -\Gamma_p[\,\sigma_{13}(\nu_p)N_1(z) + \sigma_{45}(\nu_p)N_4(z) - \sigma_{54}(\nu_p)N_5(z)\,]P_p(z) \quad (9)$$

$$\frac{dP_s(z)}{dz} = \Gamma_s[\,\sigma_{21}(\nu_s)N_2(z) - \sigma_{12}(\nu_s)N_1(z)\,]P_s(z) \quad (10)$$

2.2. Analytical Solutions to the Rate Equations

The multilevel rate equations (Eqs.(1)-(7)) for the EYCDFA system is obtained under steady-state conditions, i.e., dNi/dt=0 and are simplified to

$$\frac{\sigma_{12}(\nu_s)P_s(z)\Gamma_sN_1(z)}{A_ch\nu_s} + \frac{\sigma_{13}(\nu_p)P_p(z)\Gamma_pN_1(z)}{A_ch\nu_p} - \frac{\sigma_{21}(\nu_s)P_s(z)\Gamma_sN_2(z)}{A_ch\nu_s} - \frac{N_2(z)}{t_{21}} + \frac{\sigma_{45}(\nu_p)P_p(z)\Gamma_pN_4(z)}{A_ch\nu_p} - \frac{\sigma_{54}(\nu_p)P_p(z)\Gamma_pN_5(z)}{A_ch\nu_p} - \frac{N_5(z)}{t_{54}} = 0 \quad (11)$$

2.2.1 Signal gain

From Equations (4), (7), (9), (10) and (11) we obtain

$$\frac{1}{A_ch\nu_p}\frac{dP_p(z)}{dz} + \frac{1}{A_ch\nu_s}\frac{dP_s(z)}{dz} + \frac{N_2(z)}{t_{21}} + \frac{N_5(z)}{t_{54}} = 0 \quad (12)$$

By defining $\eta_0 = N_2/(N_2 + N_5)$ as the initial energy transfer efficiency [9], that is, $N_5 = ((1-\eta_0)/\eta_0)N_2$, and letting $B = (\tau_{21}\,\tau_{54})/(\tau_{54} + \tau_{21}(1-\eta_0)/\eta_0)$, Eq.(12) can be rewritten as

$$N_2(z) = -B\frac{1}{A_ch\nu_p}\frac{dP_p(z)}{dz} - B\frac{1}{A_ch\nu_s}\frac{dP_s(z)}{dz} \quad (13)$$

Setting $S = \int_0^z N_2(z)dz$, and then integrating Eqs. (9), (10) and (13), we get

$$S = \frac{\frac{1}{\Gamma_p}\ln\frac{P_p(z)}{P_p(0)} + \sigma_{13}N_{Er}z + \sigma_{45}N_{Yb}z}{\sigma_{13} + (1-\eta_0/\eta_0)(\sigma_{45}+\sigma_{54})} \quad (14)$$

$$S = \frac{\frac{1}{\Gamma_s}\ln\frac{P_s(z)}{P_s(0)} + \sigma_{12}N_{Er}z}{(\sigma_{12}+\sigma_{21})} \quad (15)$$

$$S = -B\frac{1}{A_ch\nu_p}[P_p(z) - P_p(0)] - B\frac{1}{A_ch\nu_s}[P_s(z) - P_s(0)] \quad (16)$$

From Equations (14) and (15), we get

$$P_p(z) = P_p(0)\left[\frac{P_s(z)}{P_s(0)}\right]^{\alpha}\exp[\alpha\Gamma_s\sigma_{12}N_{Er}z - \Gamma_pz(\sigma_{13}N_{Er} + \sigma_{45}N_{Yb})] \quad (17)$$

Where

$$\alpha = \frac{\Gamma_p\sigma_{13}+\Gamma_p(\sigma_{45}+\sigma_{54})(1-\eta_0)/\eta_0}{\Gamma_s(\sigma_{12}+\sigma_{21})}$$
(18)

Manipulating Eqs. (15), (16) and (17), we can arrive at the following equation

$$\left[\frac{P_p(z)}{P_p(0)}\right]^{1/\alpha}\exp[\Gamma_s\sigma N_{Er}z] = 1-\frac{\nu_s P_p(0)}{\nu_p P_s(0)}\left[\frac{P_p(z)}{P_p(0)}-1\right]-\frac{\ln[P_p(z)/P_p(0)]+\alpha\Gamma_s N_{Er}z(\sigma+\sigma_{12})}{\alpha B\Gamma_s(\sigma_{12}+\sigma_{21})}\frac{A_c h\nu_s}{P_s(0)}$$
(19)

$$[G(z)]^{\alpha}\exp[-\alpha\Gamma_s\sigma N_{Er}z] = 1-\frac{\nu_p P_s(0)[G(z)-1]}{\nu_s P_p(0)}-\frac{\ln G(z)+\Gamma_s\sigma_{12}N_{Er}z}{B\Gamma_s(\sigma_{12}+\sigma_{21})}\frac{A_c h\nu_p}{P_p(0)} \quad (20)$$

With $G(z) = P_s(z)/P_s(0)$

$$\sigma = \frac{\sigma_{12}+\sigma_{21}}{\sigma_{13}+(\sigma_{45}+\sigma_{54})(1-\eta_0)/\eta_0}\left(\sigma_{13}+\sigma_{45}\frac{N_{Yb}}{N_{Er}}\right)-\sigma_{12}$$
(21)

Where G(z) is the gain of the amplifier.

2.2.2 Pump threshold

Parameter	Symbol	Value	Unit
Pump wavelength	λp	980	nm
Signal wavelength	λs	1550	nm
Er concentration	NEr	1.0x1026	m-3
Yb concentration	NYb	2.0x1027	m-3
Er3+ absorption cross-section	σ13	2.58x10-25	m2
Yb3+ absorption cross-section	σ45	1.0x10-24	m2
Yb3+ emission cross-section	σ54	1.0x10-24	m2
Er3+ absorption cross-section	σ12	6.5x10-25	m2
Er3+ emission cross-section	σ21	9.0x10-25	m2
Er3+ emission lifetime	τ21	10	ms
Yb3+ emission lifetime	τ54	2	ms
Initial energy transfer efficiency	η0	0.115	-
Core refractive index	n1	1.52812	-
Cladding refractive index	n2	1.51	-
Amplifier cross-section	Ac	16	µm2
Pump overlap factor	Γp	0.921	-
Signal overlap factor	Γs	0.795	-

When G(L) =1, the gain is called threshold value and from Eq. (20), we can express the pump threshold Pth as

$$P_{th} = P_p(0) = \frac{\sigma_{12}N_{Er}LA_c h\nu_p}{B(\sigma_{12}+\sigma_{21})[1-\exp(-\alpha\Gamma_s\sigma N_{Er}L)]}$$
(22)

2.2.3 Optimum waveguide length

When $\left.\frac{\partial G_z}{\partial z}\right|_{z=L_0} = 0$, from Eq. (20), we can express the maximum gain G0 and the optimum waveguide length L0 as follows, respectively

$$G_0(L_0) = \gamma^{1/\alpha}\exp(\Gamma_s\sigma N_{Er}L_0)$$
(23)

$$L_0(G_0) = \frac{\ln G_0-\frac{1}{\alpha}\ln\gamma}{\Gamma_s\sigma N_{Er}}$$
(24)

ISSN 2229-5518

Where

$$\gamma = \frac{A_c \sigma_{12} h\nu_p}{\alpha B \Gamma_s (\sigma_{12}+\sigma_{21}) P_p(0)\sigma}$$
(25)

Specially, when NYb = 0, then N4 = N5 = 0, in this case, the EYCDWA degenerates as an EDWA.

2.2.4 Noise figure

The noise figure, F(z), can be calculated by ASE+ noise at each point along the amplifier using Equations 20 and 23 [6],

$$F(z) = \frac{1}{G(z)} + \frac{P_{ASE+}(z,\nu_s)}{G(z) h\nu_s \Delta\nu_s}$$
(26)

Where 1/G(z) is the shot noise, vs is the signal frequency, and $\Delta\nu_s$ is the noise bandwidth used to measure the powers PASE.

3. Results and Discussion

Following the model described in previous section, Calculations are performed using Matlab programs to analyze the gain and noise figure characteristics of the phosphate glass EYCDFA and show its dependence on the transmitted signal, pump, wavelengths, Er-concentration, Yb- concentration and along the amplifier length. The values of parameters used in the calculation are selected as [10-15]:

TABLE I SUMMARIZES ALL THE PARAMETERS USED IN THE CALCULATION IN THE PRESENT ANALYSIS.

3.1 Effects of pump power on gain

Figure 1 shows the relation between the gain of EYCDFA and the inputs pump power for different value of fiber length z, where we take the signal power Ps0 = 1μW, Er3+ ion concentration NEr = 1.0×1026 m–3, Yb3+ ion concentration NYb =2.0×1026 m–3. We can see that as the input pump power increases the gain increases until reaches the saturation region. This is because the doped Yb3+ ions surround Er3+ ions and form Er3+-Yb3+ ion-ion pairs, by which the Yb3+ ion absorbed photon energy transited phonon energy, which can sufficiently transferred to Er3+ ions to make more population reversion. This means that Yb3+ ions can provide an indirect exciting way to Er3+ ions. As the pump power increases to sufficiently large, almost all the Er3+ ions have realized the population reversion, and then the gain becomes saturate. At the same condition, because the doped Yb3+ ions absorb some pump energy, this fact implies that the incorporation of Yb ions improves the efficiency of pump power.

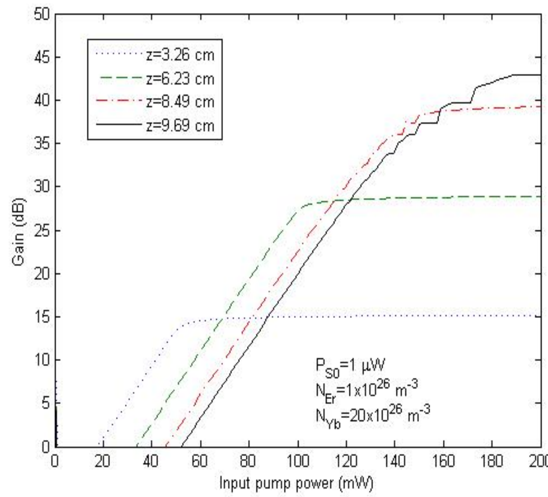

Fig. 1 the curves of the gain G versus the pump power at Ps0=1 μW

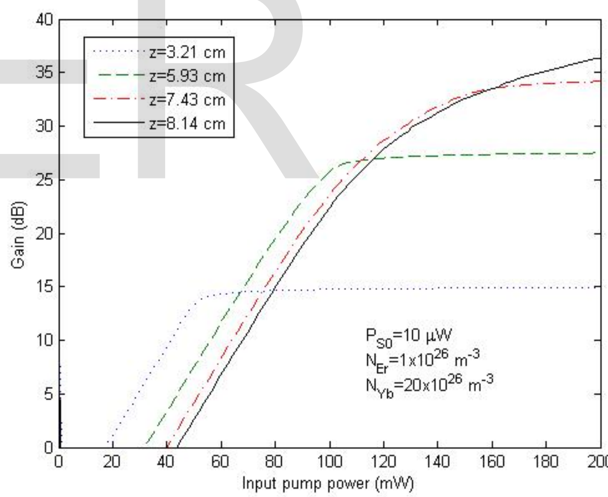

Fig. 2 the curves of the gain G versus the pump power at Ps0= 10 μW

ISSN 2229-5518

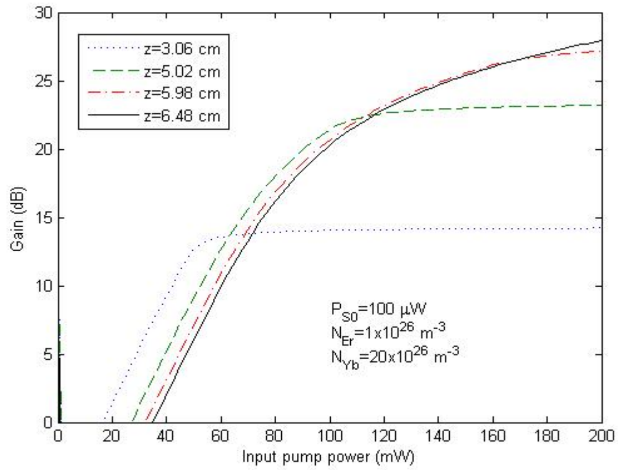

Fig. 3 the curves of the gain G versus the pump power at Ps0= 100 µW

Figures 2 and 3 show the same relation between the gain of EYCDFA and the inputs pump power for different value of fiber length z, for another two values of the signal power Ps0 = 10 and 100µW for Er3+ ion concentration NEr = 1.0×1026 m–3, Yb3+ ion concentration NYb =2.0×1026 m–3. From the behavior of the gain we conclude that as the input signal power increase, the gain increases.

3.2 Effects of the signal power on gain

Figures 4 and 5 show how the gain varies as a function of input signal power for different fiber lengths and different pumping power, Er3+ ion concentration NEr = 1.0×1026 m–3, Yb3+ ion concentration NYb = 2.0×1026 m–3. From fig. 4 for 50 mW pump power, the gain reduces sharply in highly doped fiber due to insufficient pumping and as the fiber length increase, the behavior of the curves also increase. We can observe that the easier saturation of the EYCDFA within the range of the input signal power Ps0 < 2×10–2 mW, the gain nearly keeps a constant for every curve. Beyond this, the gain decreases obviously with an increase in the input signal power. This is because stronger signal power can decrease Er3+ ion population reversion, and so the gain becomes weak. It can be seen that the saturation of gain occurs at slightly lower signal power. The comparison of the last figures, seen that for a sufficiently large pump power, the gain linearly increases. Since the amplifier reaches the population inversion, the variation in maximum gain is small despite occurring a high increase in pump power and at higher amplifier length, the gain decrease sharply.

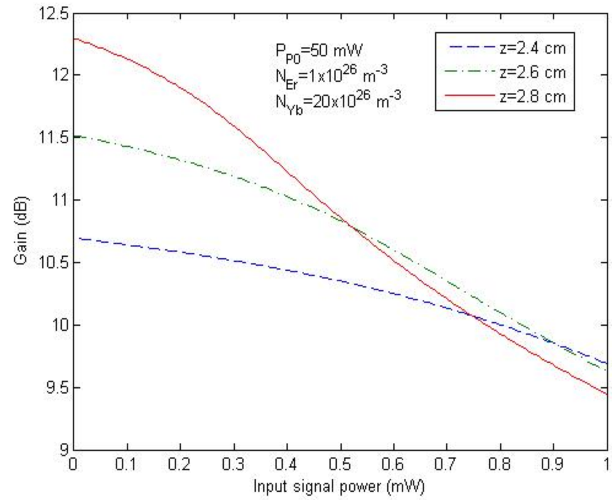

Fig. 4 the variation of gain with input signal power at PP0=50 mW

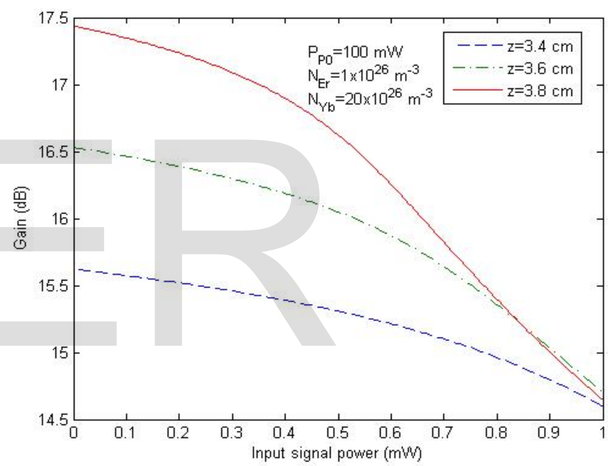

Fig. 5 the variation of gain with input signal power at PP0=100 mW

3.3 Effects of input pump power on noise figure

Figures 6, 7and 8 show the noise figure as a function of input pumping power for different signal powers 1, 10 and 100 µW , different fiber lengths and Er3+ ion concentration NEr = 1.0×1026 m–3, Yb3+ ion concentration NYb = 2.0×1026 m–3.

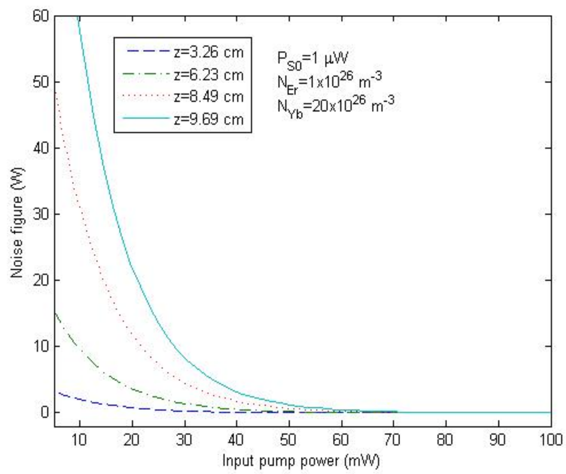

Fig. 6 NF versus input pump power at PS0=1 μW

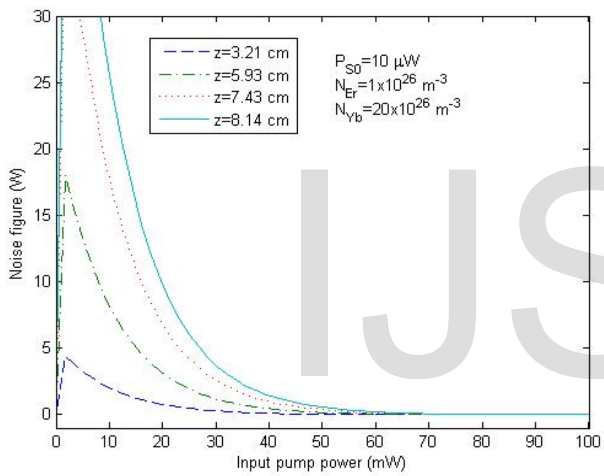

Fig. 7 NF versus input pump power at PS0=10 μW

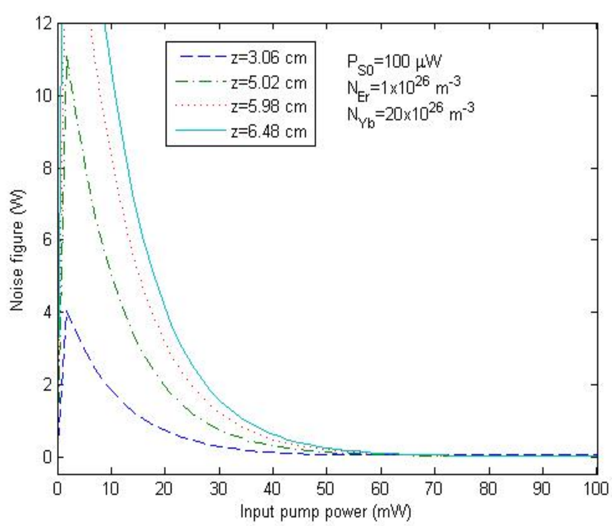

Fig. 8 NF versus input pump power at PS0=100 μW

From the figures and for a small signal power application of 1 μW, it is seen from the figure 6 that, EYCDFA shows the higher gain performance than other signal power applications because The noise figure has a smaller value than other figures 7, and 8.

As the pump power increases, the noise figure gradually decreases to a constant value for all the curves. This is because high pump power results in a strong population inversion before the gain saturates. For low pump power, high noise figure is observed because the gain is low, the noise figure of the EYCDFA varies linearly with ASE power and inversely with the amplifier gain as in Eq. (1). For a fixed pump power, as the fiber length increases the noise figure also increases at the first region and then for second region the noise figure decrease, confirming that it is more difficult to maintain a high level inversion for long fiber length compared to short length [14, 15].

4- Conclusion

We have demonstrated a computational method for calculating the properties of phosphate glass Er3+-Yb3+-co-doped waveguide amplifiers (EYCDFA). Several parameters have important effects on gain and noise figure of EYCDFA, like the variations of signal and pump power. The calculation performed using the rate equations and the light propagation equations under the uniform dopant and the steady-state condition. On the basis of preceding analysis and discussion for the gain and noise figure characteristics of the phosphate glass EYCDFA, some conclusions are reached as follows.

The sensitization of Yb3+ ions can effectively restrain the Er3+ ion clusters, and reduce up-conversion nonlinear side effect. This can increase the total gain; therefore, the performance of the EYCDFA is better than that of the EDFA. Furthermore, the introduction of Yb3+ ions can shorten the length; this is propitious to the miniaturization and the integration of the EYCDFA device. In a comparison between a phosphate glass and a typical silicate glass amplifier, it was shown that the phosphate glass amplifiers exhibit higher gains than the silicate glass ones. The gain increases and noise figure decreases as the input power increase whereas the gain increases and noise figure increases as the signal power increase for our case of calculations.

REFERENCES

[1] MA LN, HU ZL, HU YM, LI ZZ. Study on upconversion fluorescence of Er3+-doped fiber amplifier pumped at 980 nm. Chinese Journal of Lasers 2005;32(11):1463–8.

[2] LU ZG, LIU JR, SUN FG, XIAO GZ, LIN P. A hybrid fiber amplifier with 36.9-dBm output power and 70-dB gain. Optics Communications 2005;256(4–6):352–7.

[3] Strohhofer C, Polman A. Relationship between gain and Yb3+ concentration in Er3+–Yb3+ doped waveguide amplifiers. J Appl Phys 2001;90:4314–20.

[4] Jin GL, Shao GW, Mu H, Hu LL, Li Q. Gain and noise figure of a double-pass waveguide amplifier based on Er/Yb-doped phosphate glass. Chin Phys Lett 2005;22:2862–4.

[5] Zhang XZ, Liu K, Mu SK, Tan CZ, Zhang D, Pun EYB, et al. Er3+–Yb3+ co-doped glass waveguide amplifiers using ion exchange and field-assisted annealing. Opt Commun 2006;268:300–4..

[6] SHOOSHTARI A, TOUAM T, NAJAFI SI, SAFAVI-NAEINI S, HATAMI-HANZA H. Yb3+ sensitized Er3+-doped waveguide amplifiers: a theoretical approach, Optical and Quantum Electronics 1998;30(4):249–64.

[7] Yu-Hai Wang, Chun-Sheng Ma, De-Lu Li, Da-Ming Zhang. Effects of pumped styles on power conversion efficiency and gain characteristics of phosphate glass Er3+–Yb3+-co-doped waveguide amplifier. Optics & Laser Technology 2009;41:545–549.

[8] YU-HAI WANG, CHUN-SHENG MA, DE-LU LI, DA-MING ZHANG. Formulized analytical technique for gain characteristics of phosphate glass Er3+/Yb3+ co-doped waveguide amplifiers. Optica Applicata 2008;38(2):329-339.

[9] GRUBB SG, HUMER WF, CANNON RS, WINDHORN TH, VENDETTA SW, SWEENEY KL, LEILABADY PA, BARNES WL, JEDRZEJEWSKI KP, TOWNSEND JE. +21 dBm erbium power amplifier pumped by a diode-pumped Nd:YAG laser. IEEE Photonics Technology Letters 1992;4(6):553–5.

[10] JIANG C, ZENG QJ. Optimization of erbium-doped waveguide amplifier. Optics and Laser Technology 2004;36(2):167–71.

[11] De-Long Zhang, Dun-Chun Wang, Edwin Y. B. Pun. Numerical Analysis of Optical Amplification in Er3+–Yb3+ Codoped Ti:LiNbO3 Strip Waveguides. IEEE JOURNAL OF QUANTUM ELECTRONICS 2005;41(7):958-969.

[12] Husein AHM, El-Astal AH, EL-Nahal FI. The gain and noise figure of Yb–Er-codoped fiber amplifiers based on the temperature-dependent model. Optical Materials 2011;33:543–548.

[13] Shufeng LI, Chengren LI, SONG C. Theoretical and experimental research on Er-doped and Yb-Er co-doped Al2O3 waveguide amplifiers. Optoelectron China 2008;1(3–4):329–335.

[14] Lu ZG, Lavigne A, Lin P, Grover CP. A erbium/ytterbium co-doped double-cladding fiber amplifier with 36.4-dBm output power. Proceedings of SPIE 2004; 5577:180-185.

[15] Berkdemir C, Özsoy S. Numerical analysis of the signal gain and noise figure of Yb3+-sensitized Er3+-doped fiber amplifiers at different pumping power configurations. Optical Materials 2008;31:229–232.